



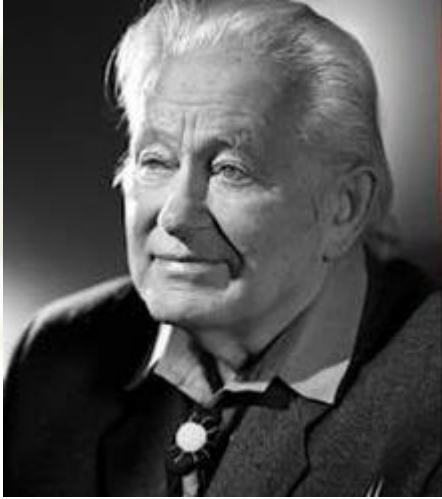
气体探测器

祝成光，山东大学



Outline

- ❖ Introduction of gas detector
- ❖ How is signal produced
- ❖ How is signal processed



1992年诺贝尔物理学奖,
法国乔治·恰帕克(Georges Charpak),
表彰他在多丝正比室的发明和发
展上所做出的杰出贡献. 气体丝室
是第一个快粒子探测器

1927年C.T.R.威尔逊(发明云室),

1948年P.M.S.布莱克特(发展云室技术并应用于原子核
和宇宙辐射研究)

1950年C.F.鲍威尔(发展乳胶技术并发现 π 介子),

1960年D.A.格兰塞尔(发明气泡室)

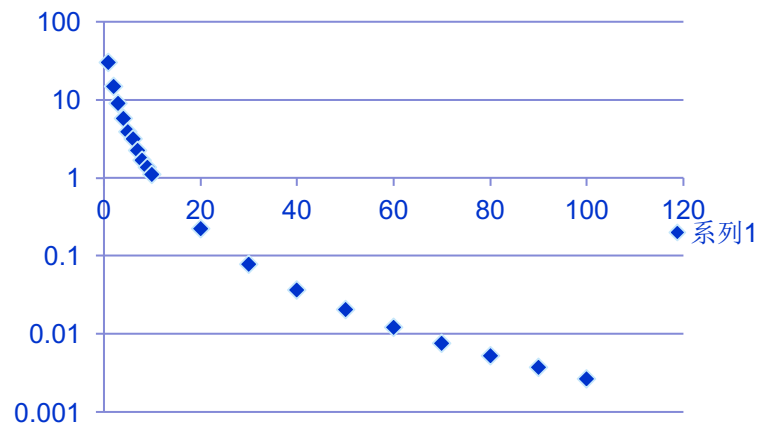
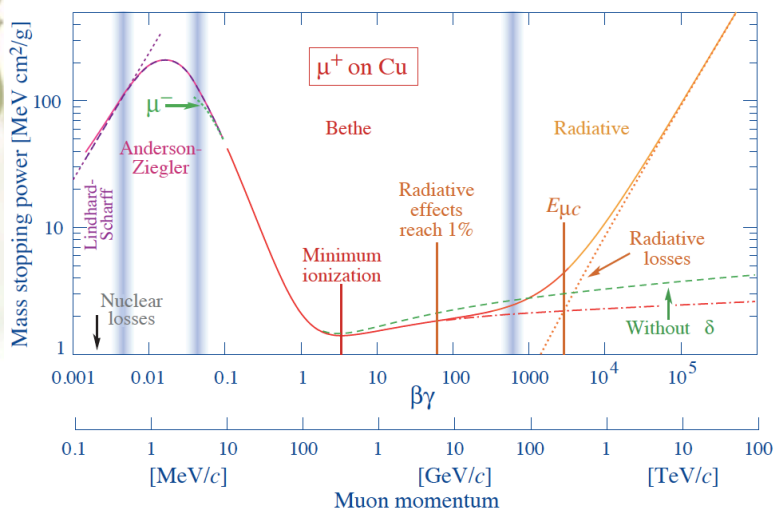
1968年L.W.阿瓦兹(发展气泡室技术)

Gas detectors

- Wire Chambers
 - Drift Chambers, MDT
 - MWPC, TGC, sTGC
 - Time Projection Chambers
- RPC, MRPC
- Well detector
- GEM detectors
- Micromegas Detectors
- Ionization of gas molecules, the released electron produce avalanche to produce microscopic signal

Condense Detectors:

- similar principle as gas detector
- Liquid Ar detector
- Si- Detectors
- No avalanche



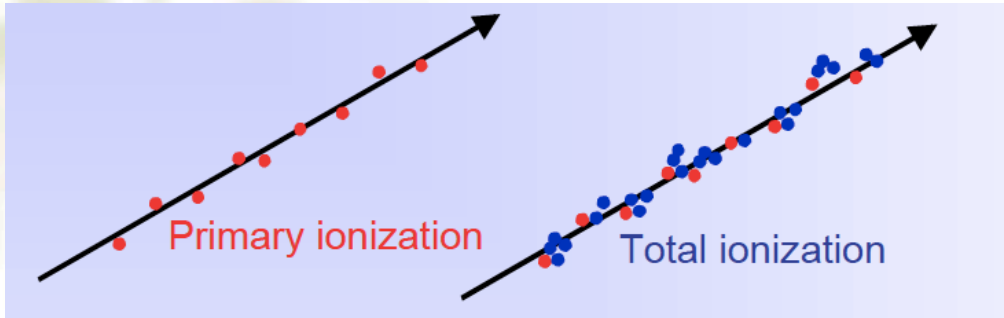
地面宇宙线muon能量分布

❖ Energy loss (ionization and excitation) between $\beta\gamma=0.1\sim 1000$ is described by Bethe formula with an accuracy of a few percent.

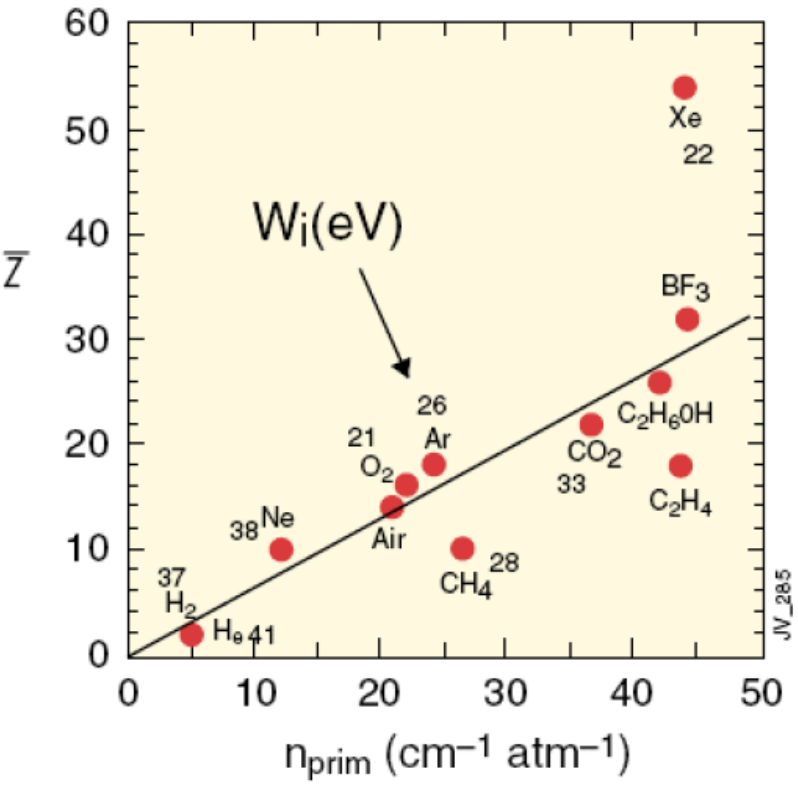
- ✓ 90% collision loss energy less than 100eV, higher energy electrons kick out is call δ -electron.
- ✓ Only function of particle velocity and charges.

❖ Minimum ionization partical(MIP): when $\beta\gamma\approx 3.2$, energy loss reach minimum. To define the detection efficiency, we normally refer to MIP efficiency.

❖ At the lower limit, the projectile velocity becomes comparable to atomic electron “velocities”, and at the upper limit radiative effects begin to be important



Molecules ionization



$$n_{total} = \frac{\Delta E}{W_i} = \frac{dE}{dx} \Delta x$$

n_{total} - number of created electron-ion pairs

$$n_{total} \approx 3...4 \cdot n_{primary}$$

ΔE = total energy loss
 W_i = effective <energy loss>/pair

Number of primary electron/ion pairs in frequently used gases

For thin gas detectors

The actual number of primary electron/ion pairs produced is Poisson distributed, thin gas detectors efficiency may be lower than 100%, $\varepsilon_d = 1 - P_0^n = 1 - e^{-n}$

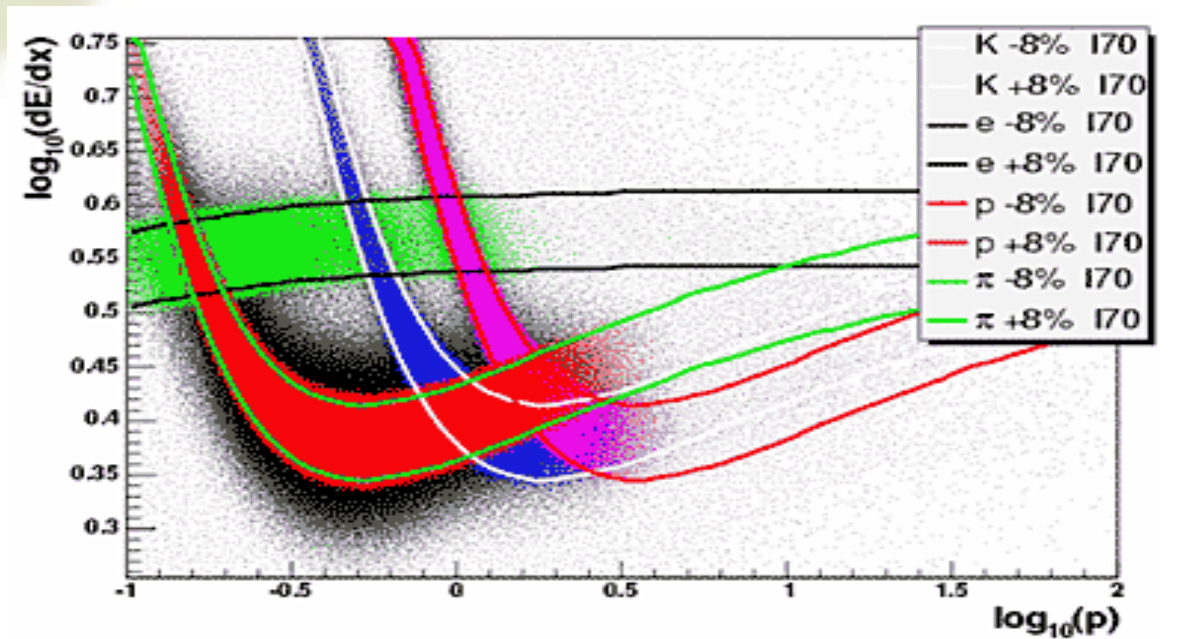
For example, for 1 mm layer of Ar $n = 2.5 \rightarrow$ efficiency = 0.92

Due to the energy loss in each collision is different:

$$T_{\max} = \frac{2m_e c^2 \beta^2 \gamma^2}{1 + (m_e / M)^2 + 2(m_e / M) \cdot \gamma} \quad P(E) = k \cdot \frac{Z}{A} \cdot \frac{x}{\beta^2 E^2} = \frac{W}{E^2}$$

the energy loss is Landau distributed with a long tail.

For particles with same momentum but different mass, the dE/dx is used to ID the particle



STAR experiment: dE/dx (keV/cm) distribution vs momentum (GeV/c). Both axes are in log scale. A 1- σ band is drawn around the center of the dE/dx for a given particle

Without electric field, the electron and ions will lose its energy, become thermal object with energy

$$\frac{3}{2}kT \approx 0.04eV$$

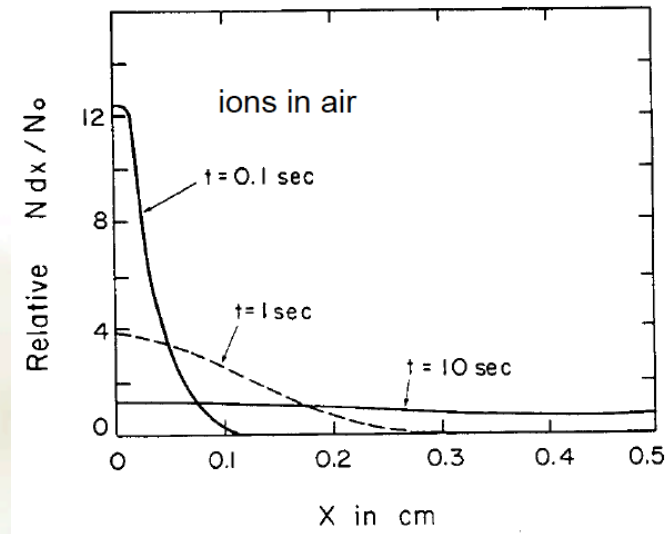
Velocity of thermal ions $10^5 cm/s$, On average, one collision happens each 100nm, meaning 10^{10} collisions per second

Free charge distribution after time t:

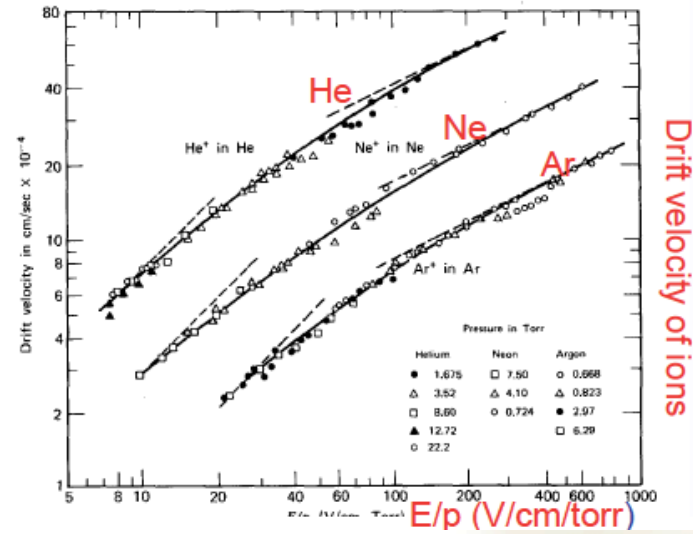
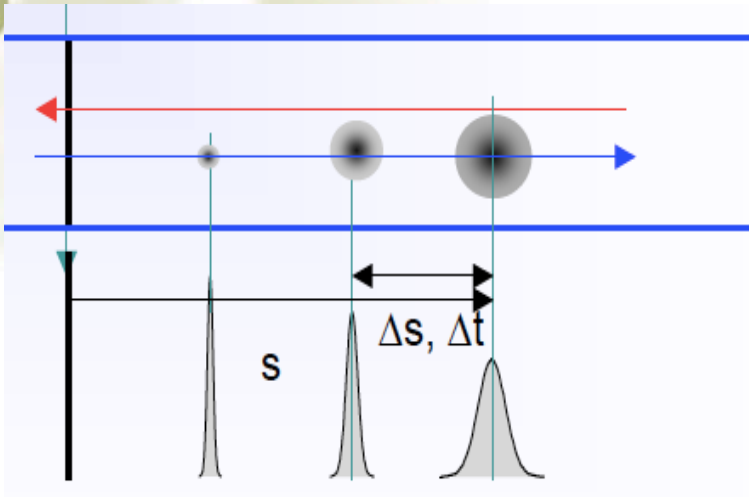
$$\frac{dN}{N} = \frac{1}{\sqrt{4\pi Dt}} \exp\left(-\frac{x^2}{2Dt}\right) dt$$

D: diffusion coefficient, at level of $0.04 cm^2/s$ in Ar

$$\sigma_x = \sqrt{2Dt}$$



Ions transportation in electric field



Drift velocity of ions is almost linear function of E $W^+ = \mu^+ \frac{E}{p}$

Mobility μ^+ is constant for given gas at fixe P and T, at level of $1\text{cm}^2/\text{vs}$

For a electric field 3000v/cm , $W^+=1\text{cm}^2/\text{vs} * 3000\text{v/cm} = 3000\text{cm/s}$

The mobility is proportional to the diffusion coefficient:

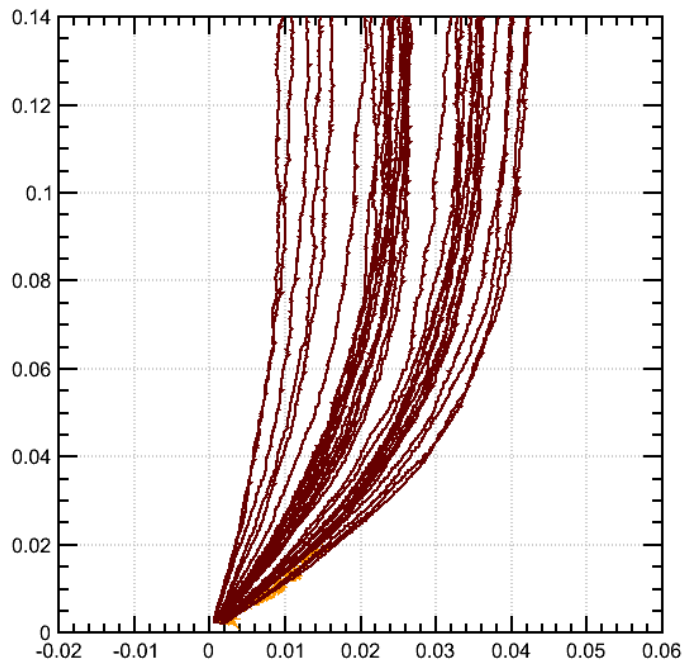
The diffusion after drift x :

$$\sigma_x = \sqrt{2Dt} = \sqrt{2D \frac{x}{W^+}} = \sqrt{2D \frac{x}{\mu^+ E}} \propto \sqrt{\frac{x}{E}}$$

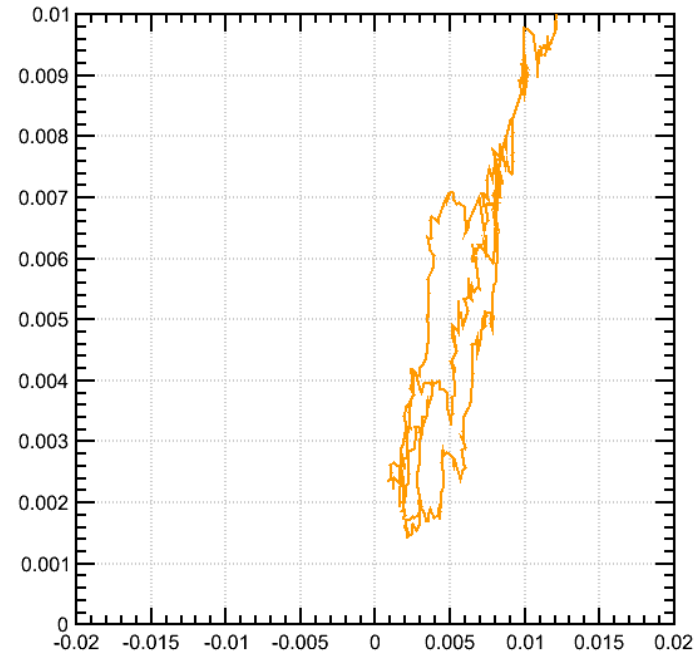
In electric field of 2000v/cm, ions diffuse 60 micros after drift 1cm. The slow ions drift along the electric lines

Electron drift and diffusion

- Electron velocity is ~ 100 times faster than ions.
- Stronger diffraction than ions, 4 times longer in mean free path
- When energy increases, the collision cross section increases and mean free path is reduced to limit the energy.



ions drift



electrons drift

❖ **Avalanche:** 100 ionized electrons created, typical noise of the amplifier ≈ 1000 e- (ENC) \rightarrow electron multiplier .

Multiplication of ionization is described by the first Townsend coefficient $\alpha(E)$, depending on the cross section of ionization of gas molecules

$$dn = n\alpha dx. \quad \alpha = \frac{1}{\lambda}. \quad \lambda: \text{mean free path.}$$

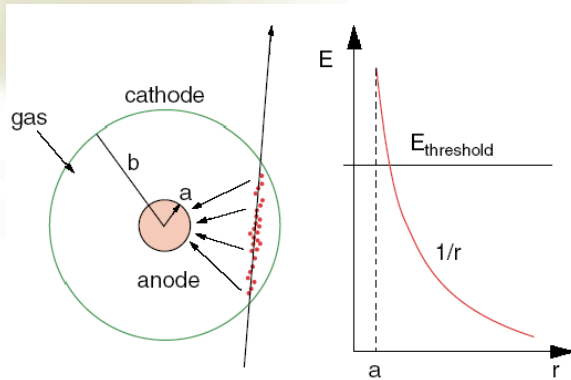
$$n = n_0 e^{\alpha(E)x}$$

$$\text{Gain: } M = \frac{n}{n_0} = e^{\alpha(E)x}$$

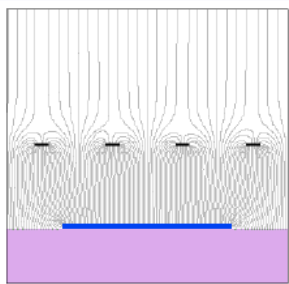
$\alpha(E)$ depends on the cross section of ionization of gas molecules and various energy transfer mechanisms.

No simple analytical expression of $\alpha(E)$, need to measure for each gas mixture, so as M

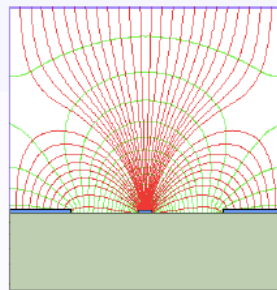
Detector types defined by avalanche method



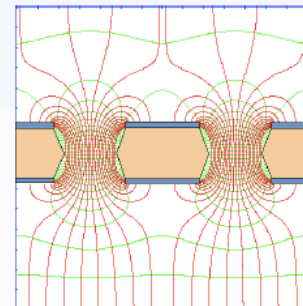
Avalanche around wire



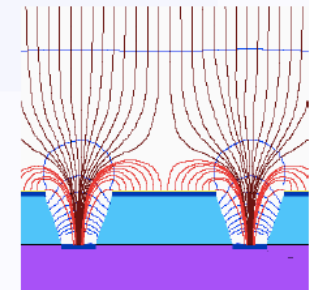
parallel plate



strip



hole



groove

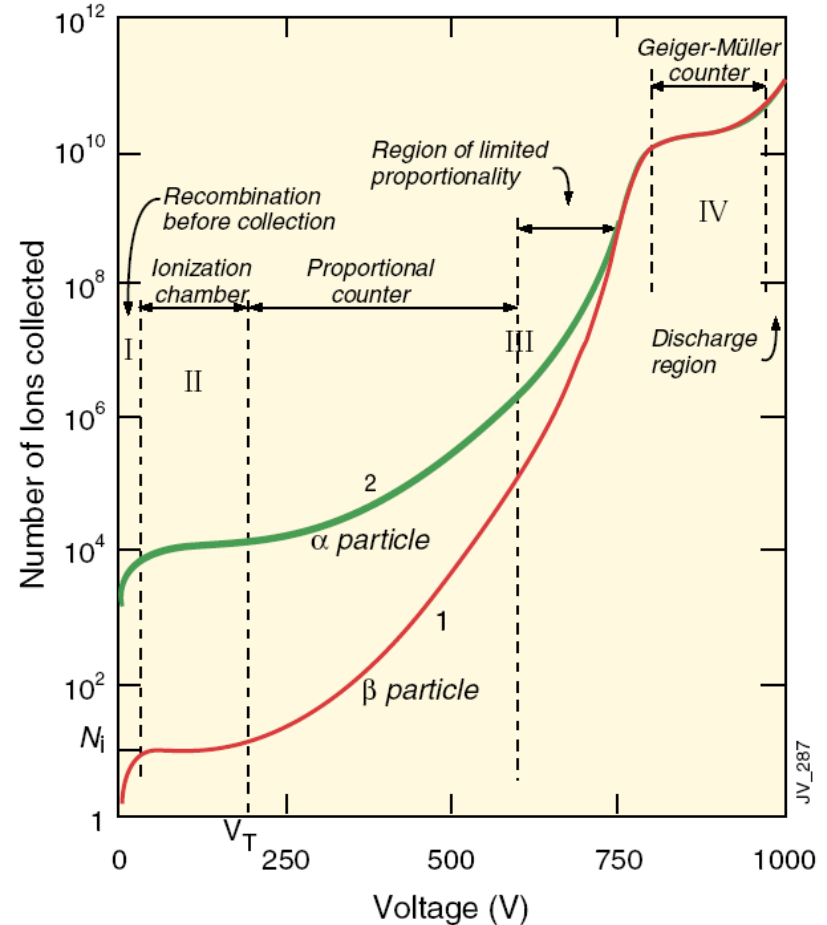
In the avalanche, molecules can be too excited and radiate photons, the photons then release electrons again from the detector materials, e.g. copper. This creates many subsequent avalanches.

Solution: add polyatomic gas as a quencher to absorb the photons in a large energy range

Disadvantage: The polyatomic molecules absorb photons will result in smaller molecules and deposit inside detector, resulting in detector ageing and fraction of quencher decrease, so most gas detectors use flowing gas.

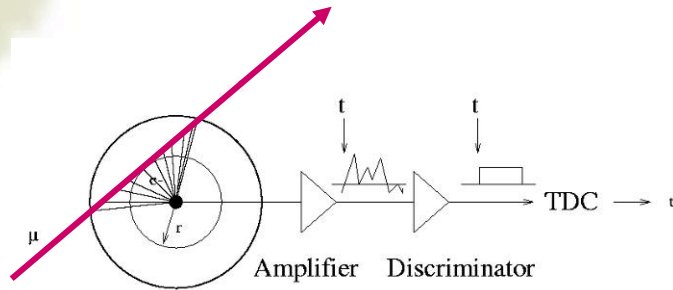
Working mode

- **ionization mode** –no charge multiplication, gain ~ 1
- **proportional mode** –signal proportional to original ionization gain $\sim 10^4 - 10^5$
- **limited proportional mode** saturated large signals, gain $\sim 10^{10}$
- **Geiger mode** –full length of the anode wire affected; discharge stopped by HV cut

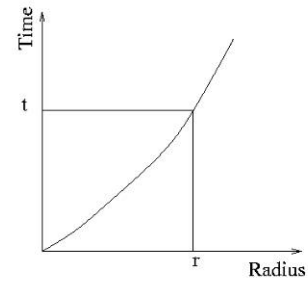


Drift Tube

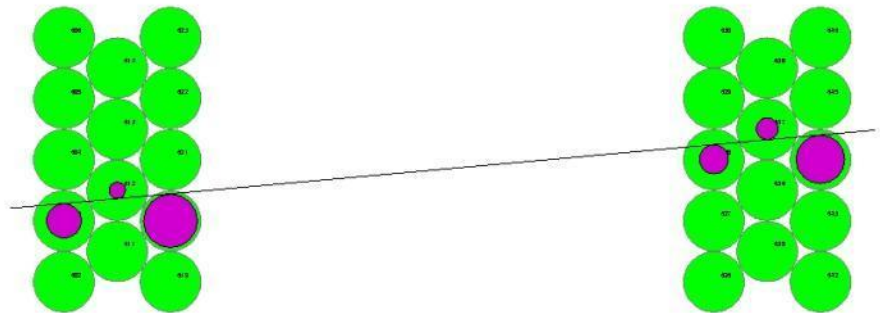
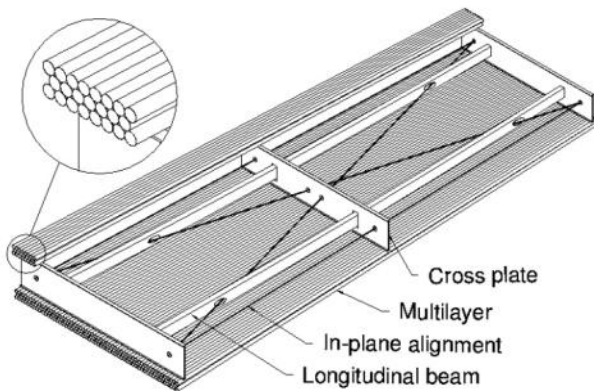
ATLAS MDT R(tube) = 15mm



Calibrated Radius-Time correlation



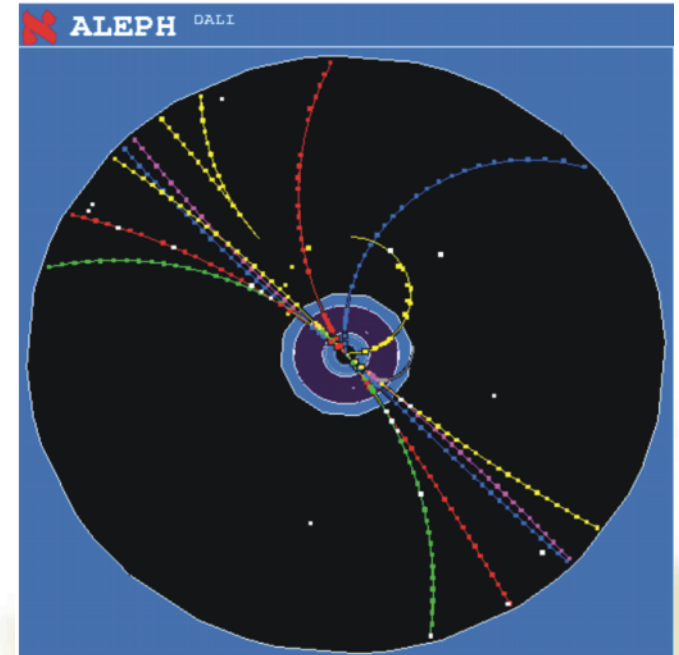
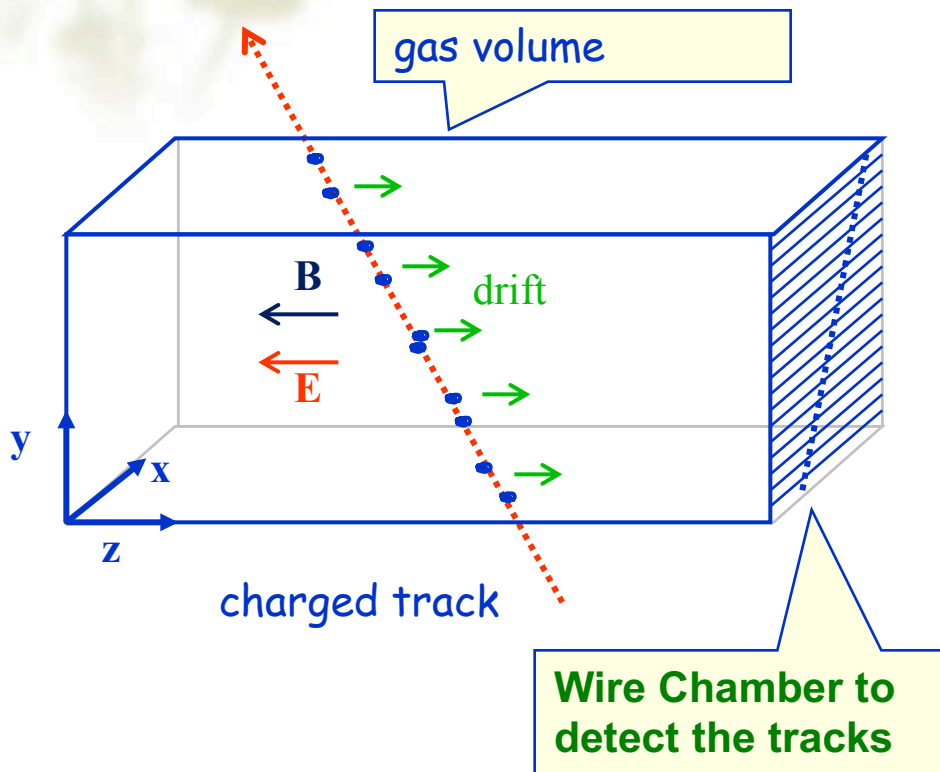
ATLAS Muon Chambers



ATLAS MDTs, 80 μ m per tube

Time Projection Chamber (TPC):

Drift Fields 100-400V/cm. Drift times 10-100 μ s.
Distance up to 2.5m !

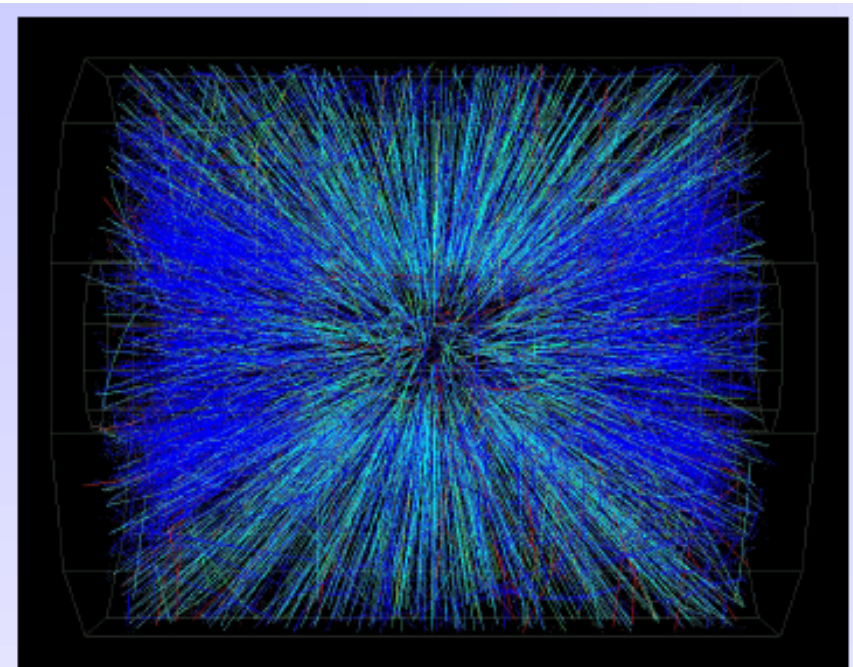
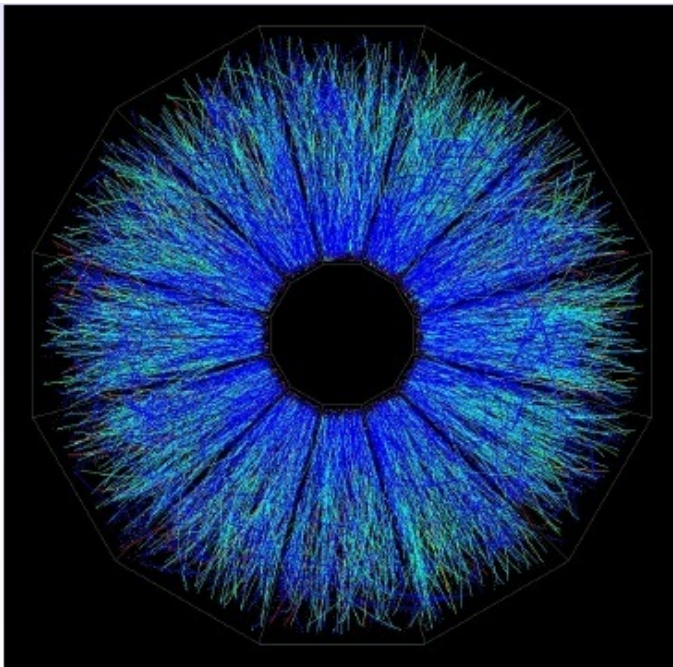


STAR TPC (BNL)

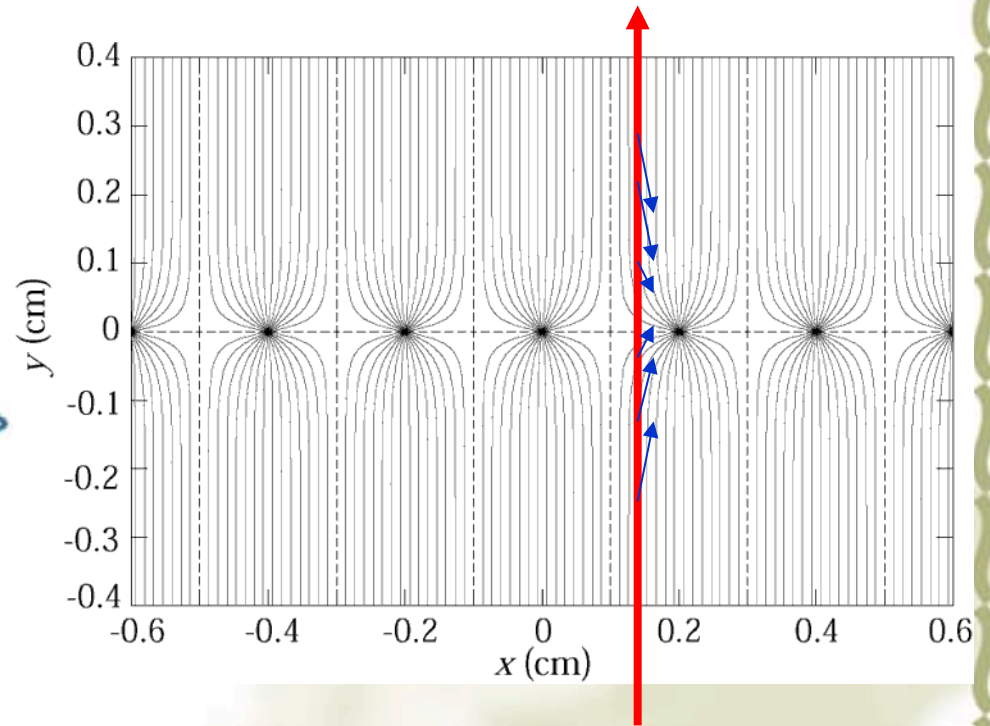
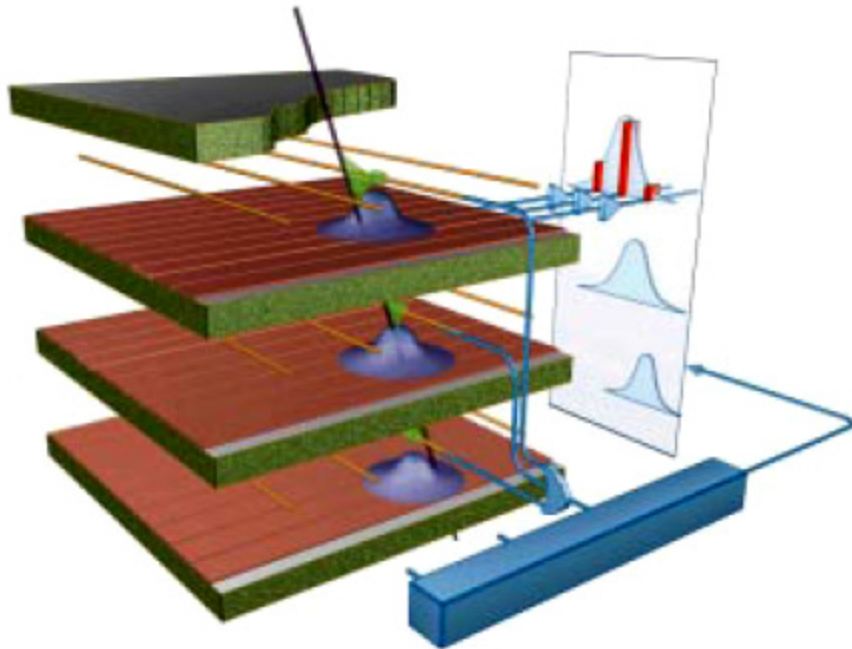
Event display of a Au Au collision at CM energy of 130 GeV/n.

Typically around 200 tracks per event.

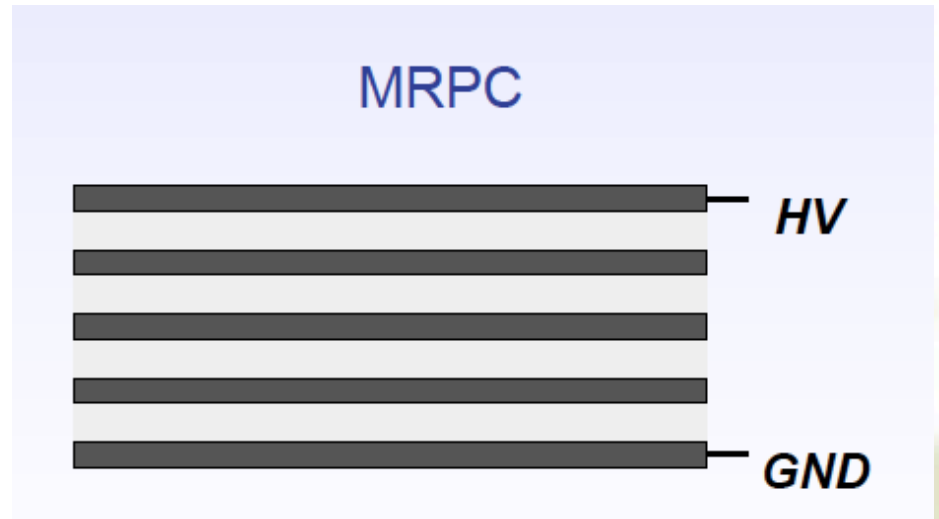
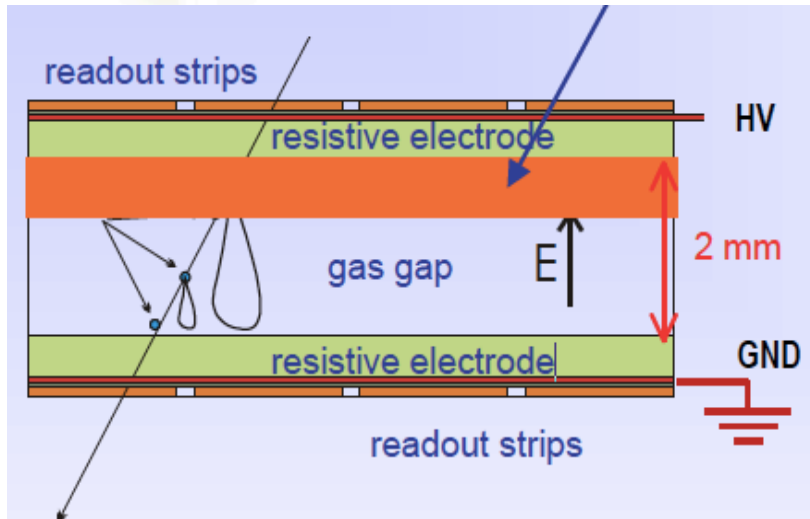
Great advantage of a TPC: The only material on the way of the particles is gas \rightarrow very low multiple scattering \rightarrow very good momentum resolution down to low momenta !



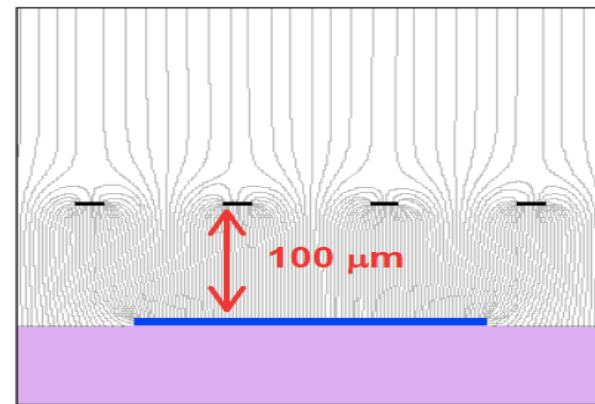
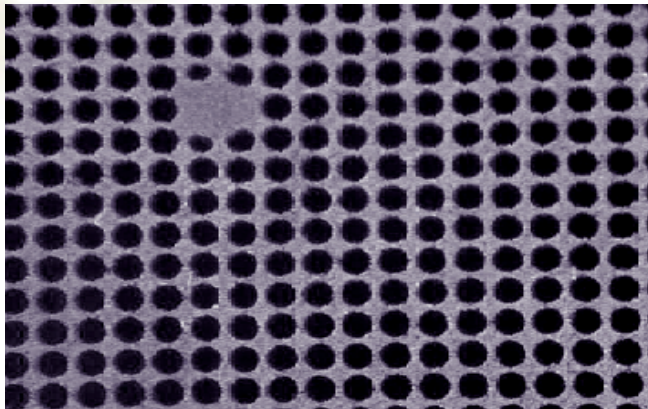
View of Wire Detector



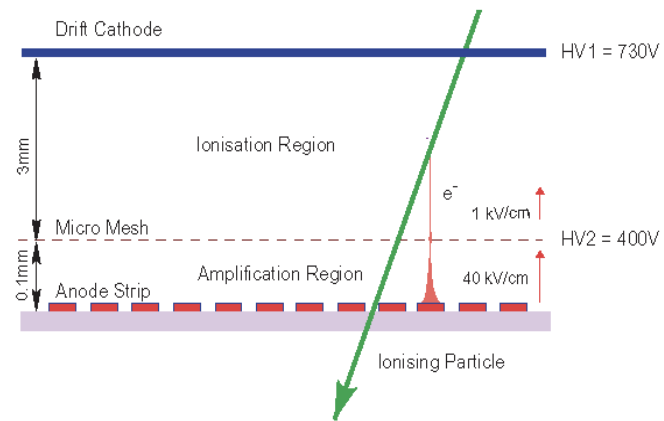
RPC, MRPC



Gas detector has many advantages, but the ions drift slow and produce space charges to degrade the performance, Micro-pattern gas detector limit the ion space.

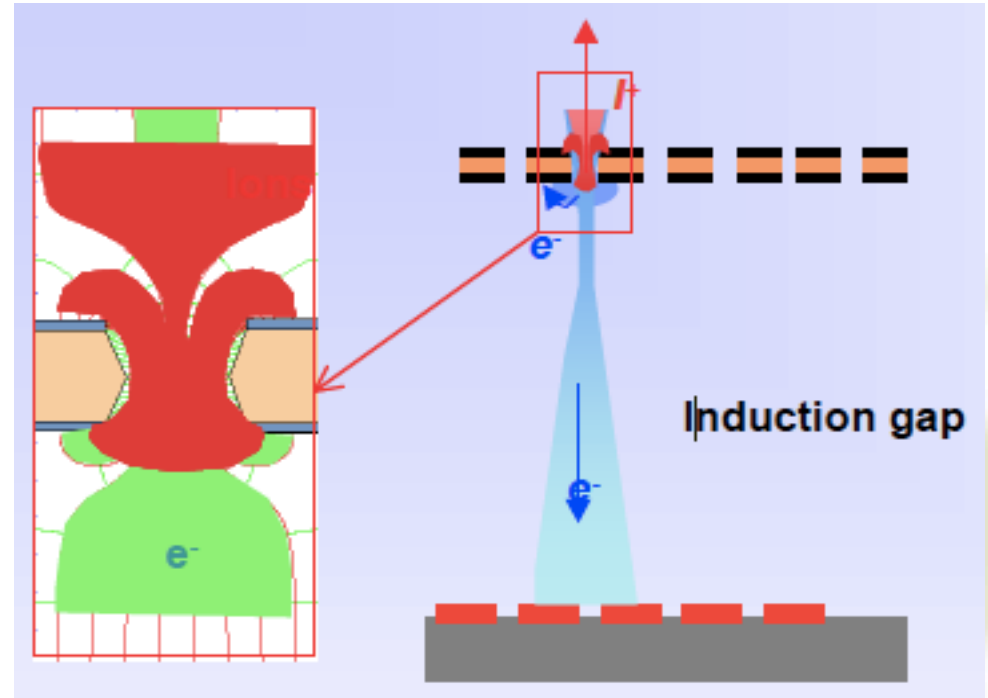
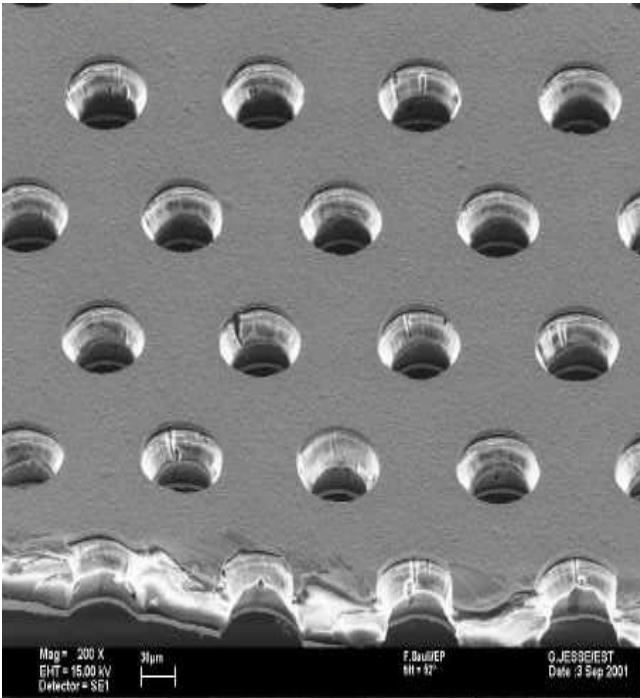
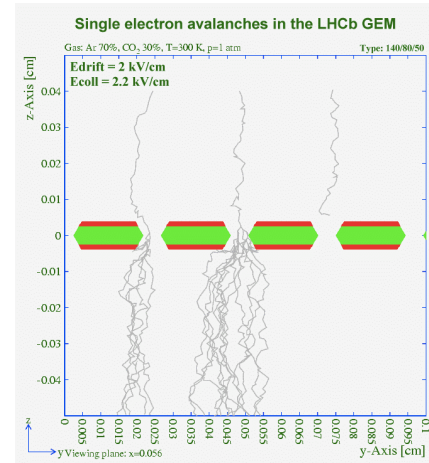


Micromegas detector



GEM detector

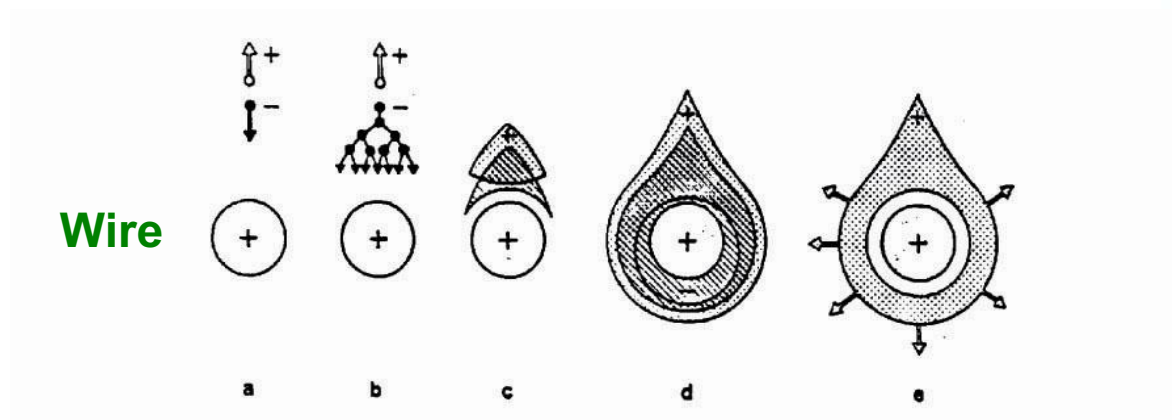
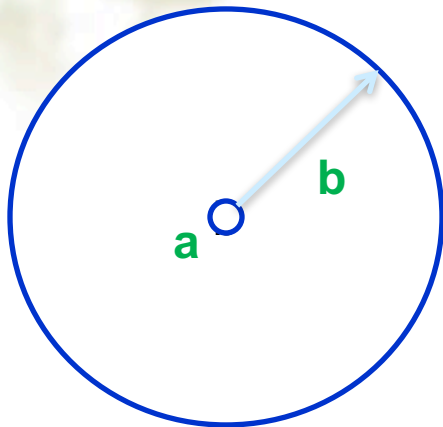
Avalanche in small holes



The background features a light cream color with faint, stylized floral illustrations in a muted greenish-yellow hue. A decorative border with a wavy, scalloped pattern in the same color runs along the right and bottom edges of the page.

How is signal produced

Electric field close to a thin wire (100-300kV/cm).
 E.g. $V_0=1000\text{V}$, $a=10\mu\text{m}$, $b=10\text{mm}$, $E(a)=150\text{kV/cm}$



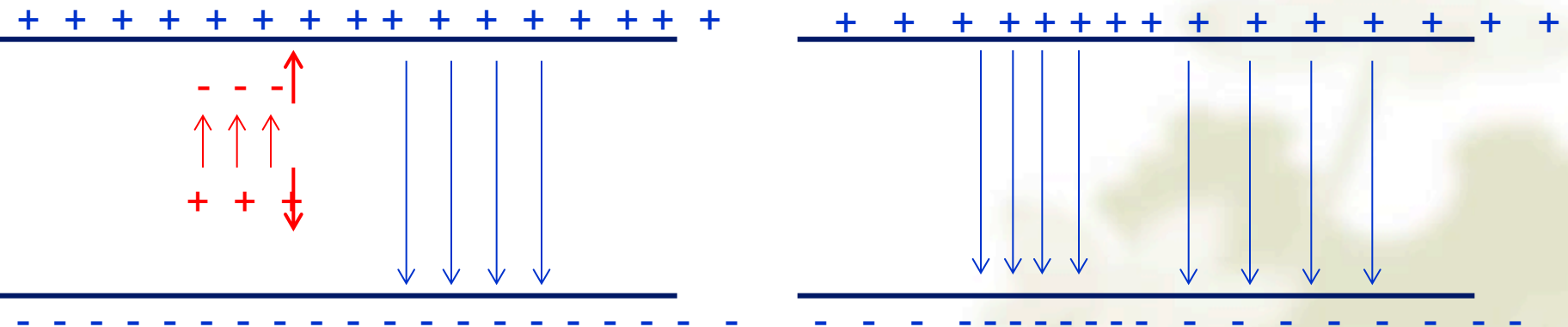
增益: $M = \frac{n}{n_0} = \exp\left[\int_{R_a}^{r_c} \alpha(r) dr\right] = \exp\left[\left(\frac{1}{\pi\epsilon_0} \cdot \sqrt{\frac{kN}{E_c}}\right) CV_0\right]$

E_c : 临界电场

一点感性认识:

1. 雪崩产生后，电子向阳极丝漂移，正电荷向阴极漂移。
2. 电荷漂移一开始，阳极板和阴极板上便分别感应出电荷。
3. 静电场环路积分为0，电荷漂移区总电场被削弱，其他区域也需要被削弱，极板上的电荷向电荷漂移区聚集。
4. 电荷漂移结束后，和极板聚集电荷中和，电容载电荷变少，电压变小，能量变少。

孤立的平板电容



V 下降: $V(t)$ depends on the how the charge drift

从能量守恒角度：

匀速分离的正负电荷导致电容上的电压差匀速降低，
电压降低的速度决定于电荷漂移的速度：

$$\frac{d}{dt}(QV + qV') = 0$$

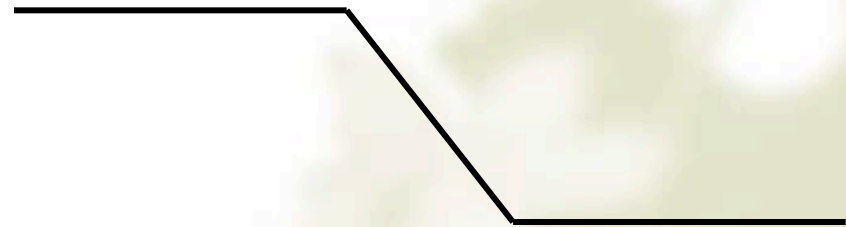
Q 电容板电荷，V 电容板电压，q 漂移电荷，
V' 漂移电荷所处的电势。

$$Q \frac{dV}{dt} = -q \frac{dEr}{dt}$$

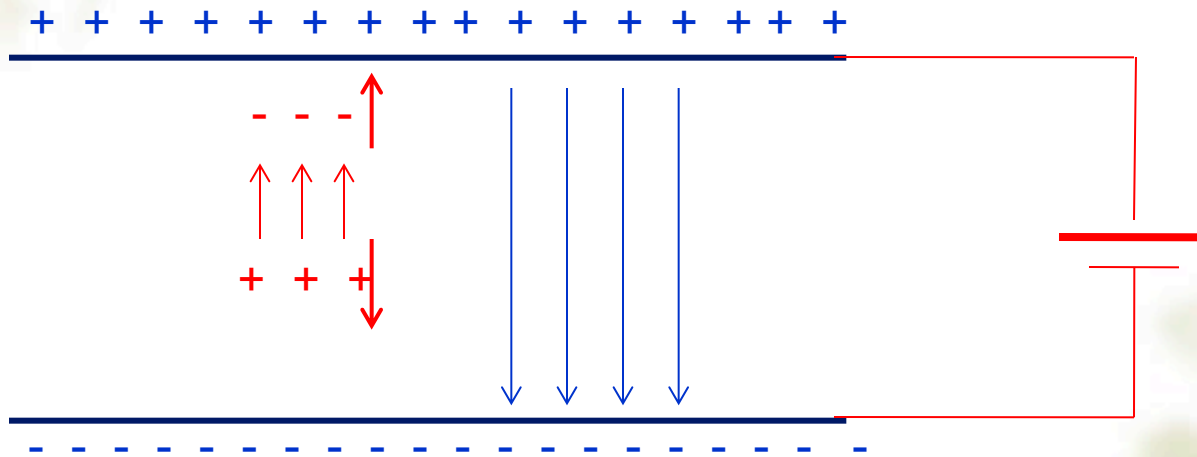
$$\frac{dV}{dt} = -\frac{qE}{Q} v$$

$$V = V_0 - \frac{qE}{Q} vt$$

孤立的平板电容



平行板有恒压源供电的情况下，
并且供电时间常数足够小



V 不变：但是有电荷向电容板上流动，流动的速度（电流）也
决定于电容之间的电荷漂移

能量守恒角度：看到有稳恒的电流向电容充电，
充电的总电荷等于漂移电荷总量（雪崩电荷）

$$\frac{d}{dt}(QV + qV') = 0$$

$$V \frac{dQ}{dt} = -q \frac{dEr}{dt}. \quad (E \text{变化很小})$$

$$i = \frac{dQ}{dt} = -\frac{qE}{V} v$$



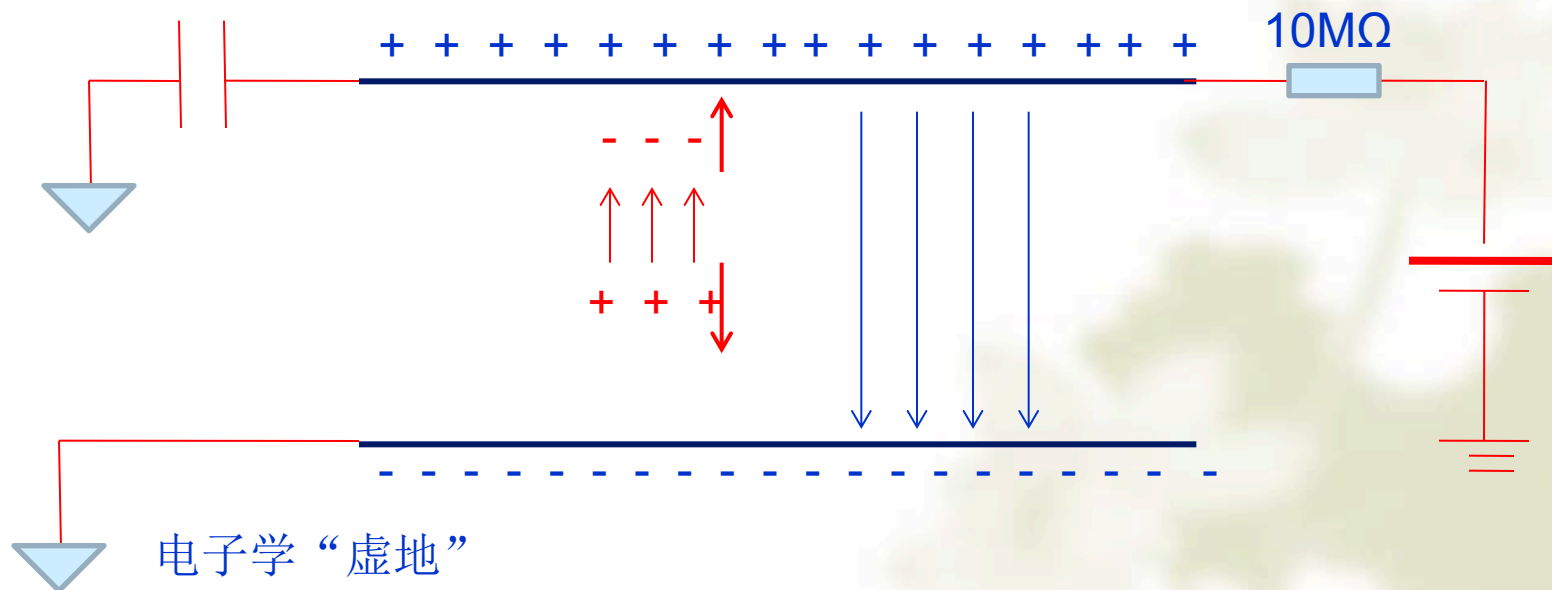
如果漂移电荷不是匀速漂移，例如阳极丝附近，那么观察到的电流信号的形状将出现更复杂的形状。

实际的探测器和高压之间串接一个大电阻（下图右），和前端电子学之间串接一个大电容（下图左），

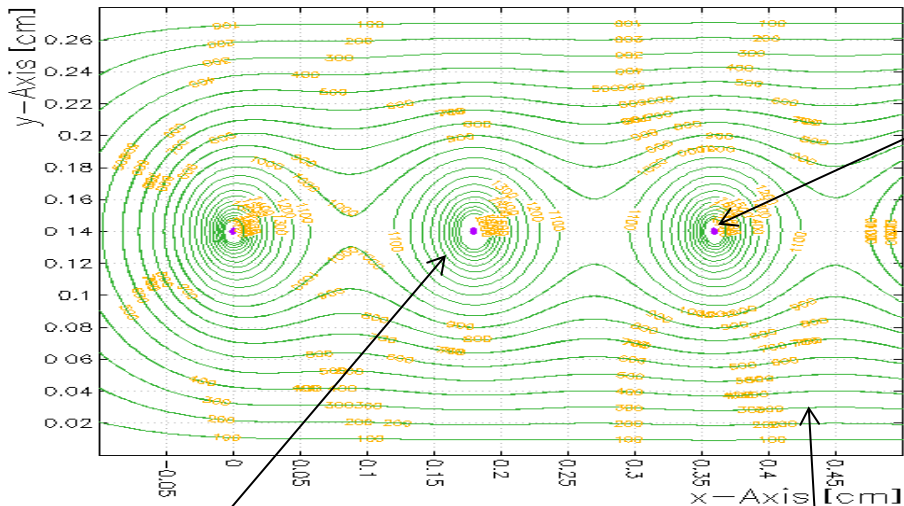
探测器内的电荷漂移通常是几十到几百ns量级，形成高频信号，可以畅通无阻的通过电容进入前端电子学，相当于恒压情况下的信号产生。

大电阻导致探测器的充电时间很长，到毫秒量级，在没有右侧电容的情况下是探测器工作在孤立状态，在有电容的情况下，在信号过后对探测器进行缓慢充电。

如果探测器工作在极高的辐射环境下，充电电流不可忽略，导致探测器的有效电压降低。



Contours of V

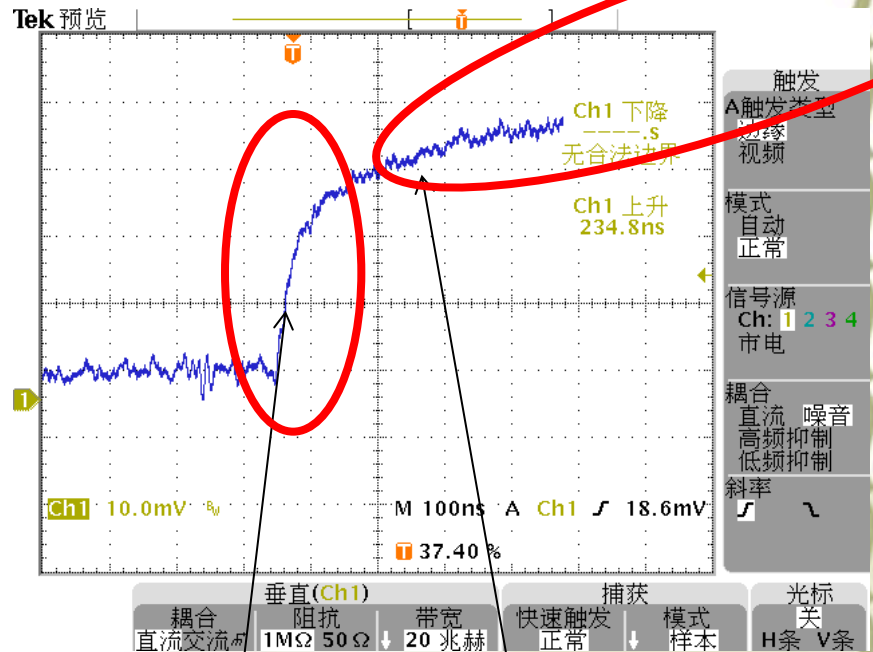


Printed at 17:49:02 on 16/04/2016 (Mathcad version 7.31)

20kv/cm. 电场放射区
 离子迁移率 $1.4 \text{ cm}^2/\text{vs}$
 速度: $1.4 \times 20 \text{ kv/cm} = 28 \text{ km/s}$
 用时: $0.5 \text{ mm} / 28 \text{ km/s} = 1700 \text{ ns}$

10kv/cm at 均匀电场区.
 离子迁移率 $1.53 \text{ cm}^2/\text{vs}$
 速度: $1.53 \times 10 \text{ kv/cm} = 15300 \text{ cm/s}$
 用时: $1 \text{ mm} / 15300 \text{ cm/s} = 6000 \text{ ns}$

300kv/cm at wire surface to
 100kv/cm at $50 \mu\text{m}$ away from wire
 离子迁移率 $0.9 \text{ cm}^2/\text{vs}$
 速度: $0.9 \times 100 \text{ k} = 90 \text{ km/s}$
 用时: $0.05 \text{ mm} / 90 \text{ km/s} = 55 \text{ ns}$

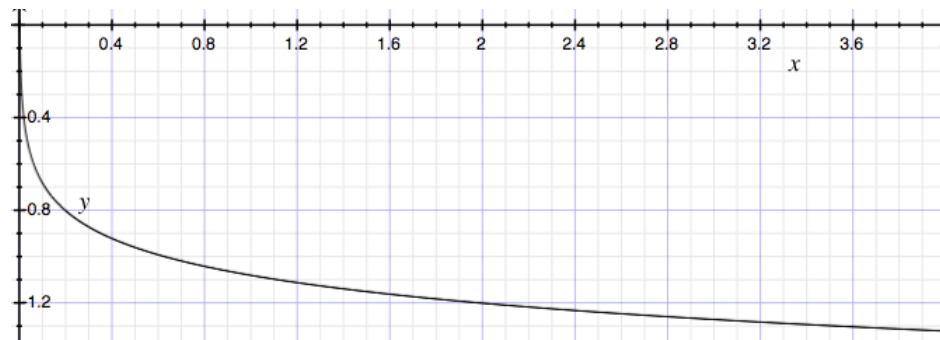


前50 微米 放射电场区漂移

$$dV = -\frac{Q}{lCV_0} dv = -\frac{Q}{lCV_0} \frac{dv}{dr} dr = -\frac{Q}{lCV_0} \frac{V_0}{\ln\left(\frac{b}{a}\right)} \frac{1}{r} dr$$

$$V(t) = -\frac{Q}{2\pi\epsilon_0 l} \ln \frac{r(t)}{R_a} = -\frac{Q}{2\pi\epsilon_0 l} \ln \frac{\sqrt{R_a^2 + \frac{\mu^+ CV_0}{\pi\epsilon_0 p} t}}{R_a} = -\frac{Q}{4\pi\epsilon_0 l} \ln\left(1 + \frac{t}{\left(\frac{\pi\epsilon_0 p R_a^2}{\mu^+ CV_0}\right)}\right)$$

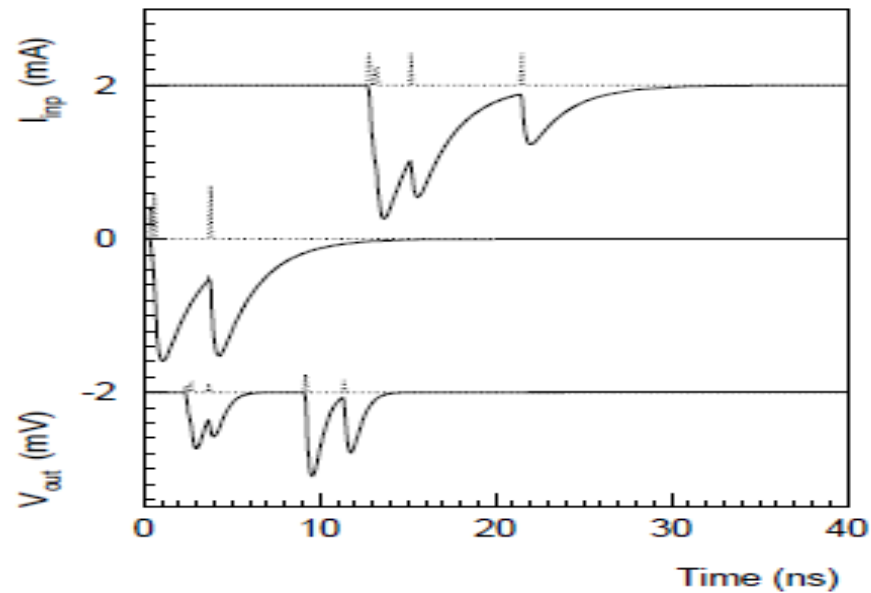
$$V(t) = -\frac{Q}{4\pi\epsilon_0 l} \ln\left(1 + \frac{t}{t_0}\right)$$



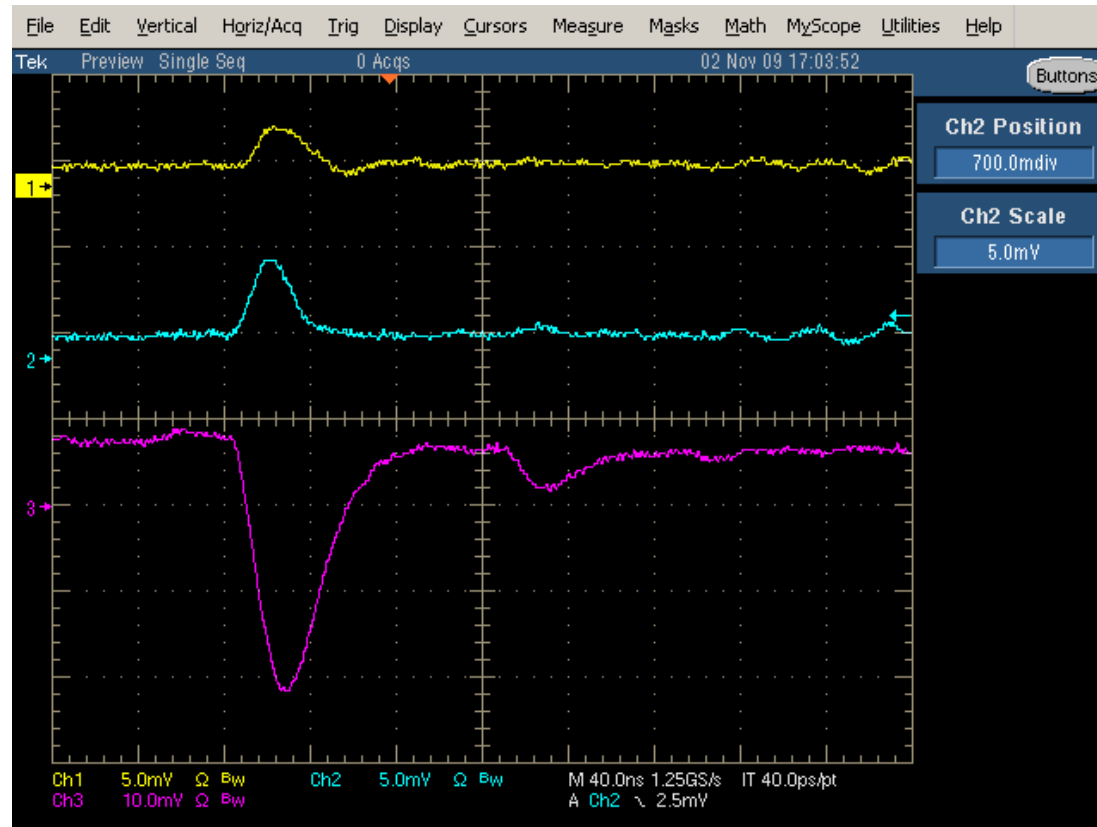
电子雪崩产生的离子向阴极漂移，经历的电场由强到弱，漂移速度先快后慢。则在上式：在阳极丝上引起的电信号先快速增加，后缓慢到达最大值。

但是因为电子学的过滤，一般几百纳秒就可以让信号尾巴消失。

- ❖ 当使用示波器观察电流时，如果示波器的输入阻抗较小（ 50Ω ），放电常数很小，上页的信号在上升到最大值之前就开始下降。



实验上观测到的探测器信号



格林倒易定理：更精确的计算感应信号

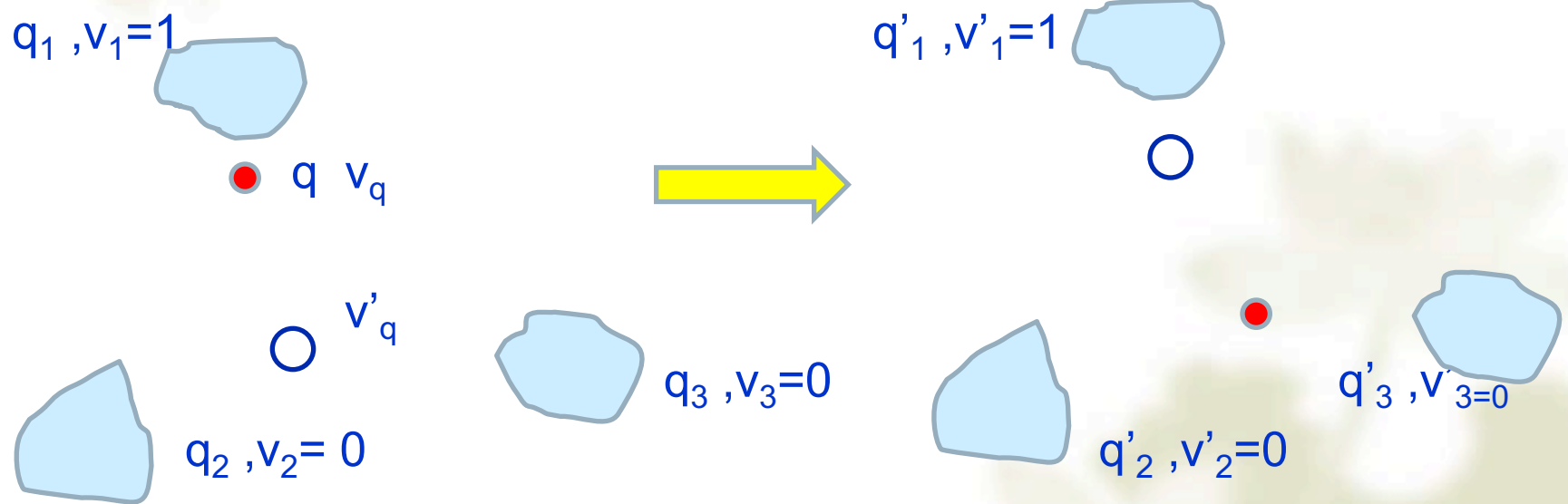
$$\begin{aligned}\int \mathbf{E}_1 \cdot \mathbf{E}_2 d^3\mathbf{r} &= -\int \nabla V_1 \cdot \mathbf{E}_2 d^3\mathbf{r} \\ -\iint \left(\int \frac{\partial V_1}{\partial x} \cdot E_{2x} dx \right) dydz &= -\iint \left(\int E_{2x} dV_1 \right) dydz \\ &= -\iint \left(E_{2x} V_1 \Big|_{-\infty}^{+\infty} - \int V_1 dE_{2x} \right) dydz \\ &= \int V_1 \frac{\partial E_{2x}}{\partial x} dx dy dz\end{aligned}$$

$$\begin{aligned}-\int \nabla V_1 \cdot \mathbf{E}_2 d^3\mathbf{r} &= \int V_1 \nabla \mathbf{E}_2 d^3\mathbf{r} = \frac{1}{\epsilon_0} \int V_1 \rho_2 d^3\mathbf{r} \\ -\int \mathbf{E}_1 \cdot \nabla V_2 d^3\mathbf{r} &= \int V_2 \nabla \mathbf{E}_1 d^3\mathbf{r} = \frac{1}{\epsilon_0} \int V_2 \rho_1 d^3\mathbf{r}\end{aligned}$$

$$\int V_1 \rho_2 d^3\mathbf{r} = \int V_2 \rho_1 d^3\mathbf{r}$$

倒易定理将两个毫不相关的
静电场联系在一起：
1. 电荷分布 ρ_1 产生电势场 V_1 .
2. 电荷分布 ρ_2 产生电势场 V_2 .

格林倒易定理的应用



感应电荷和电流: weighting field

$$qV_q + q_1 \times 1 + q_2 \times 0 + q_3 \times 0 = qV_q' + q_1' \times 1 + q_2' \times 0 + q_3' \times 0$$

$$\Delta q_1 = q_1' - q_1 = qV_q - qV_q' = -q\Delta V_q$$

$$\frac{\Delta q_1}{\Delta t} = -\frac{q\Delta V_q}{\Delta t}$$

$$i_1 = \frac{dq_1}{dt} = -q \frac{dV_q}{dt} = -q \frac{dV_q}{d\vec{r}} \frac{d\vec{r}}{dt} = q\vec{E} \cdot \vec{v}$$

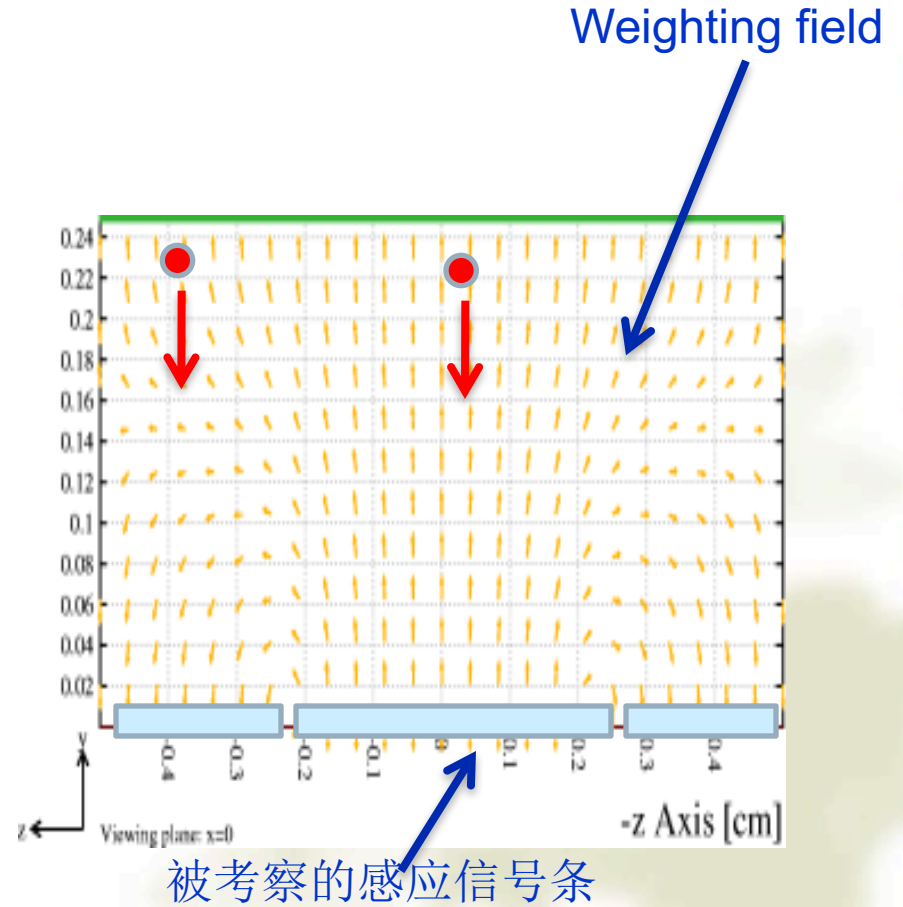
为了计算在导体1上的感应电荷（电荷变化），我们将导体1的电势设为1v，其他所有导体的电势设为0v，这样的配置所形成的电场称为 **weighting field**，通过观察移动电荷在 **weighting field** 中的移动可以精确的计算在导体1上形成的感应电流/电荷。

如果计算在导体2上的感应电荷，则需要将导体2的电势设为1，其他设为0，计算导体2的 **weighting field**。因此 **weighting field** 是一个虚拟的电场，针对每一个考察的导体，有一个 **weighting field**。

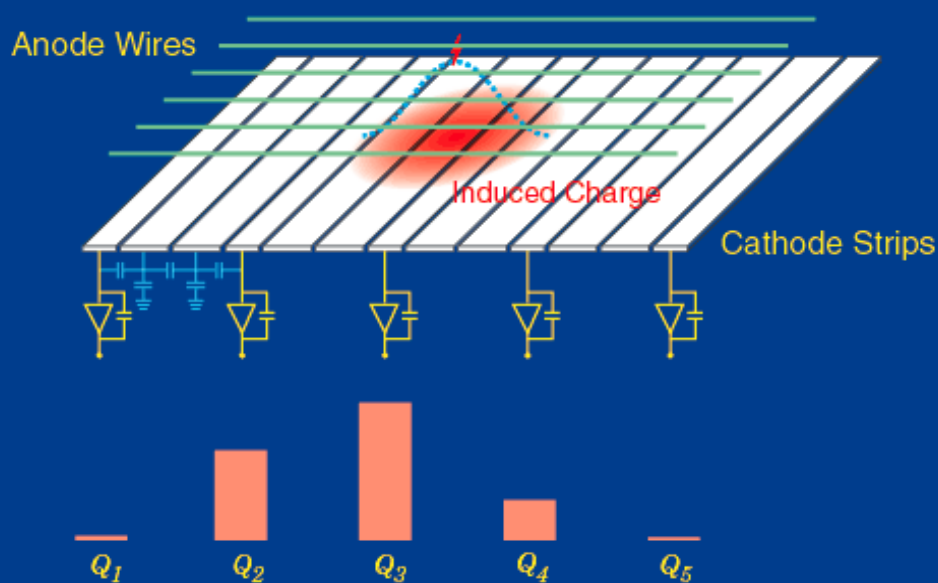
weighting field 和探测器中实际加的电场没有关系。实际电场推动电荷移动。

探测器信号的模拟

在不同的感应电极上的感应电荷是不同的。因而形成一个感应电荷的分布



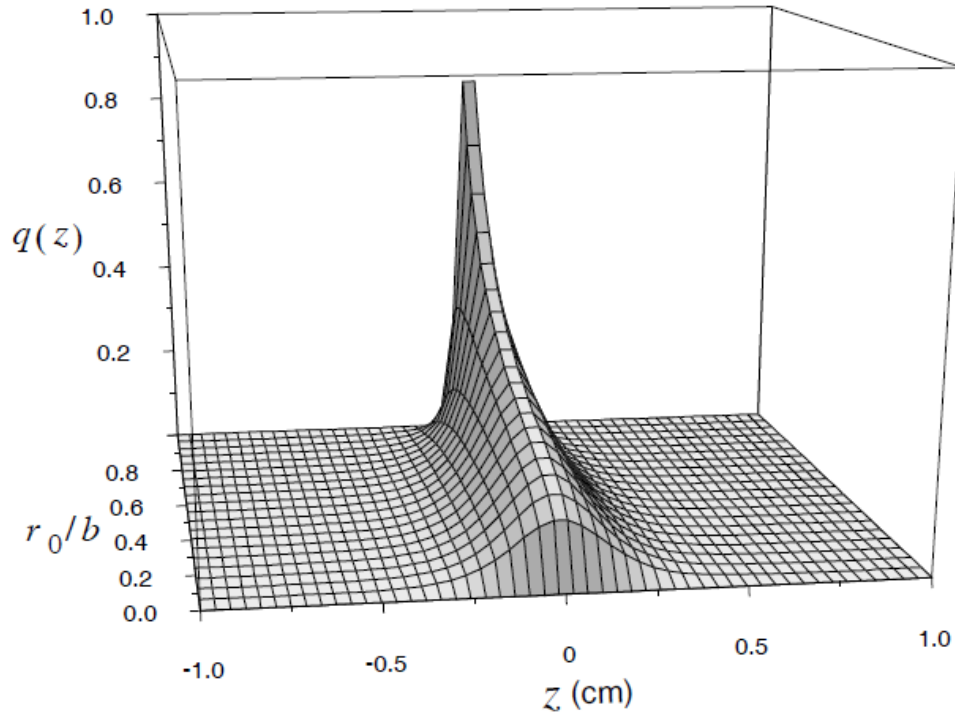
Cathode Strip Chamber (CSC) Principles of Operation



阴极面上电荷分布形状

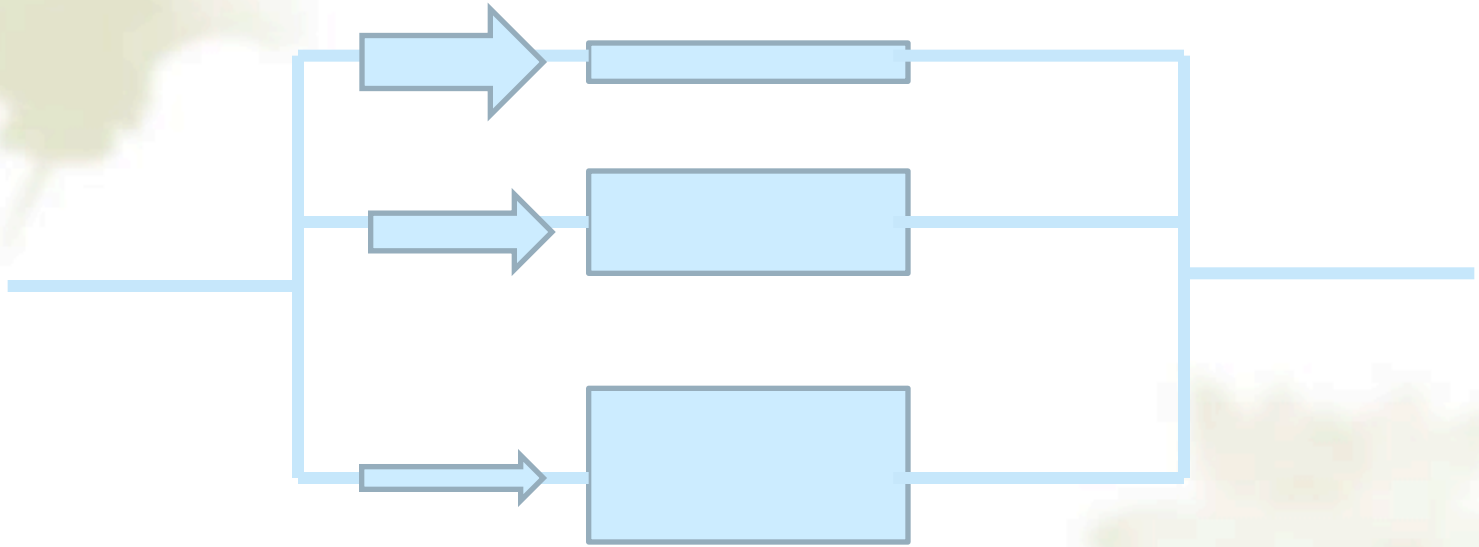
该电荷分布被分割的阴极感应条抽取成直方图，离线通过计算电荷中心来更精确的定位

staw detector



感应电荷在阴极面上的分布和漂移电荷与阳极丝的距离的关系

Current flow

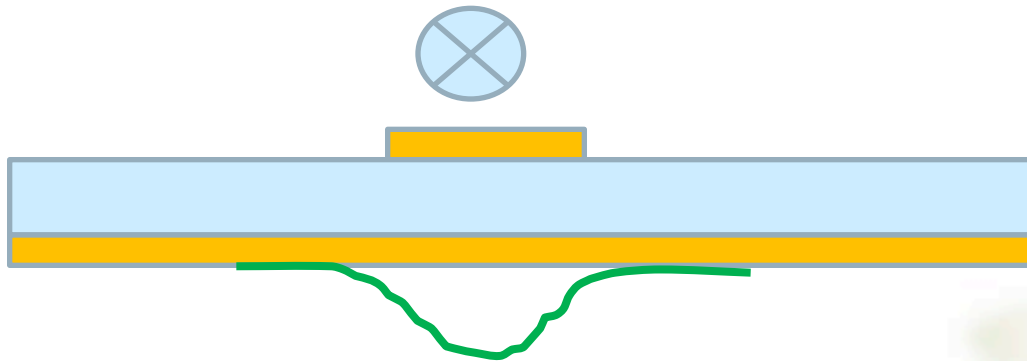


- ❖ Current flows along the low impedance path

Signal on detector

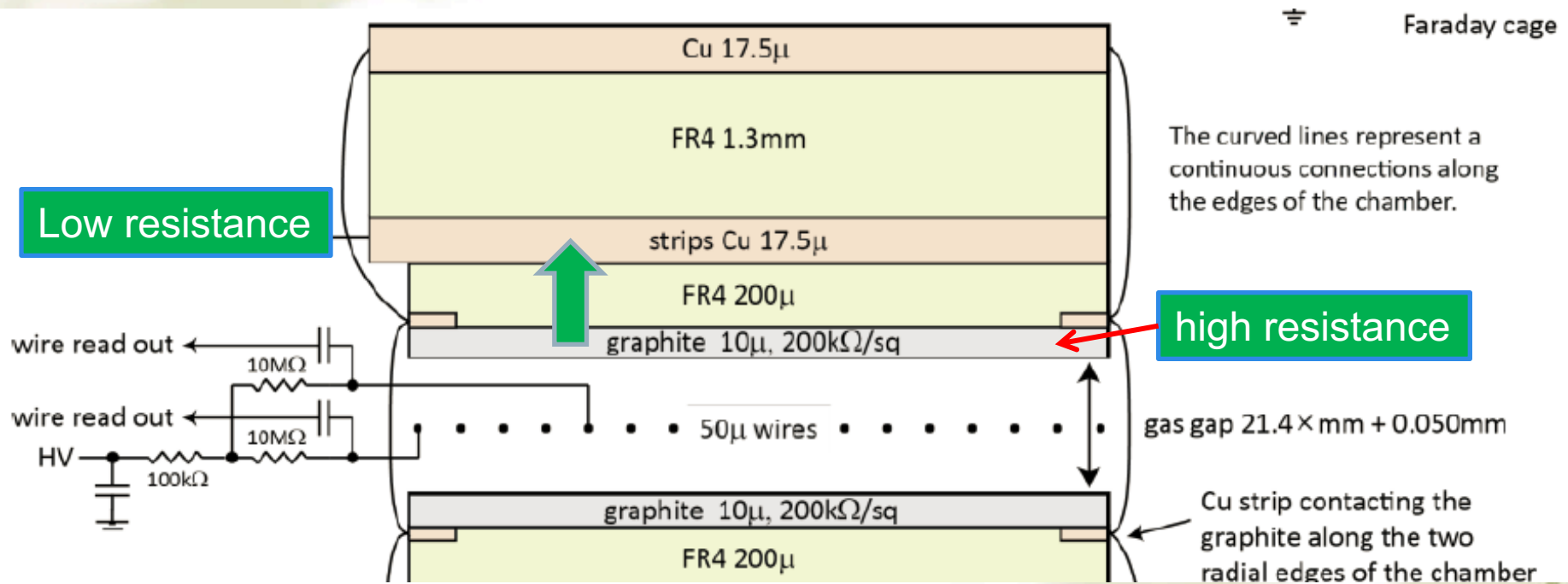
- ❖ The impedance to the signal is more complicated.
- ❖ Signal is high frequency, the impedance comes not only from resistor, but also capacitance and inductance: R , $i/\omega C$, $i\omega L$
- ❖ Signal loop choose the high capacitance and low inductance path

Low inductance path



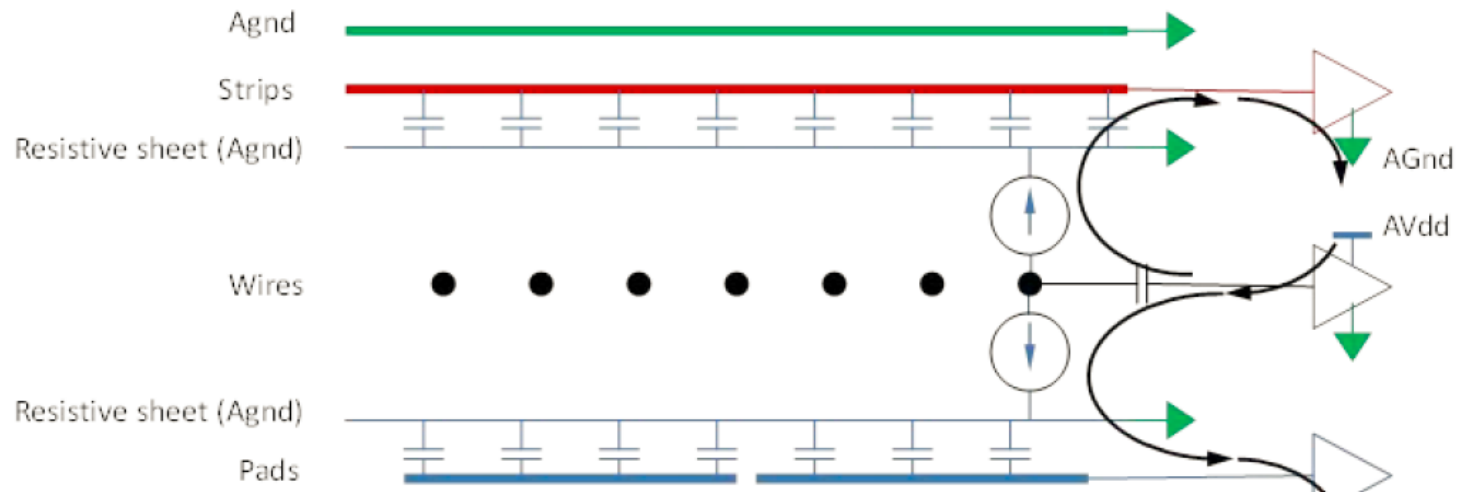
- ❖ The real path of high frequency signal are always as close to each other.

Structure of sTGC detector



- ❖ Low inductance require the area surrounded by signal path to be minimum. We need to clear the minimum inductance path for detector

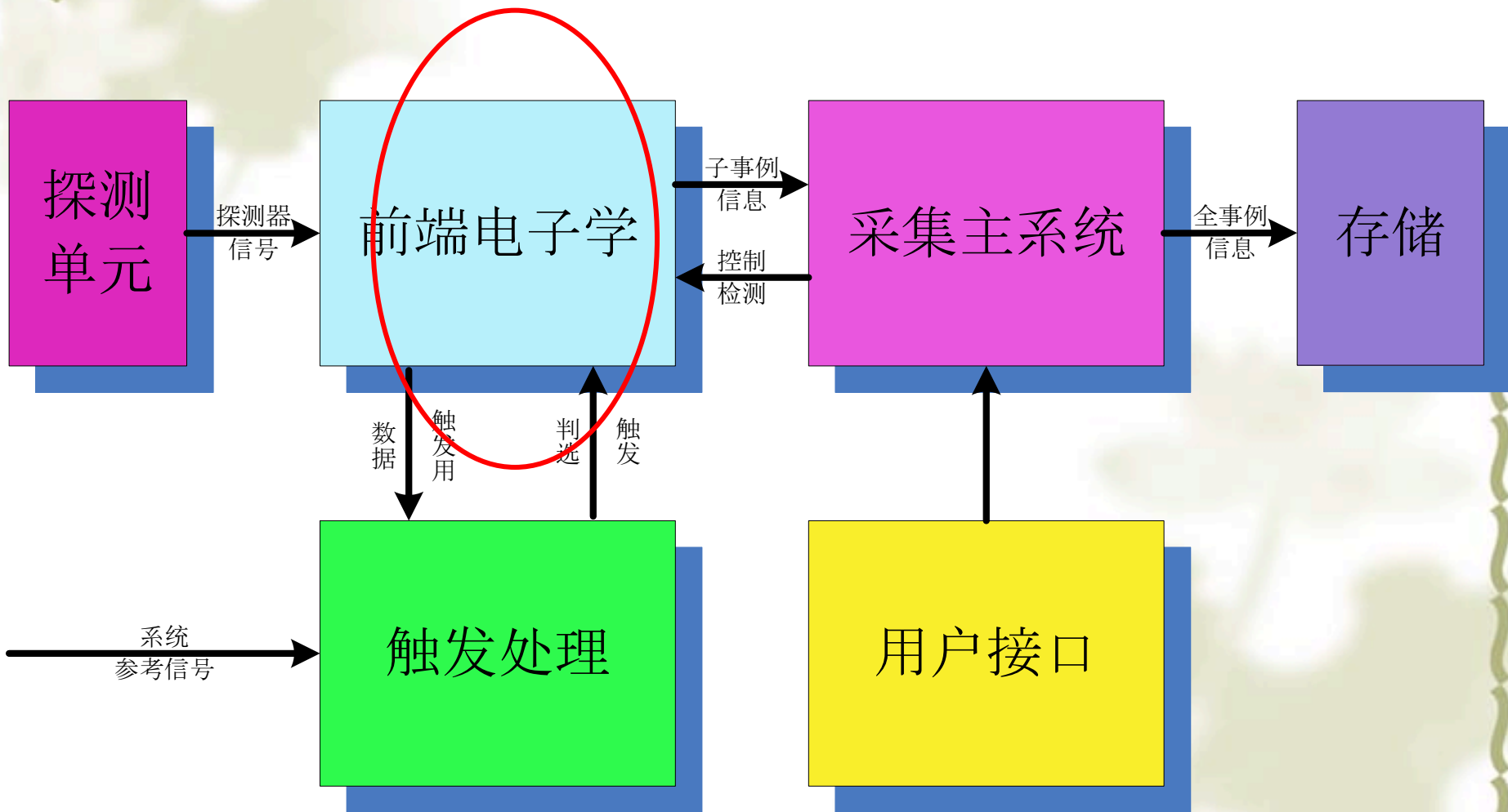
Signal flow on detector



- ❖ A complicated ground and connection is always noise source.

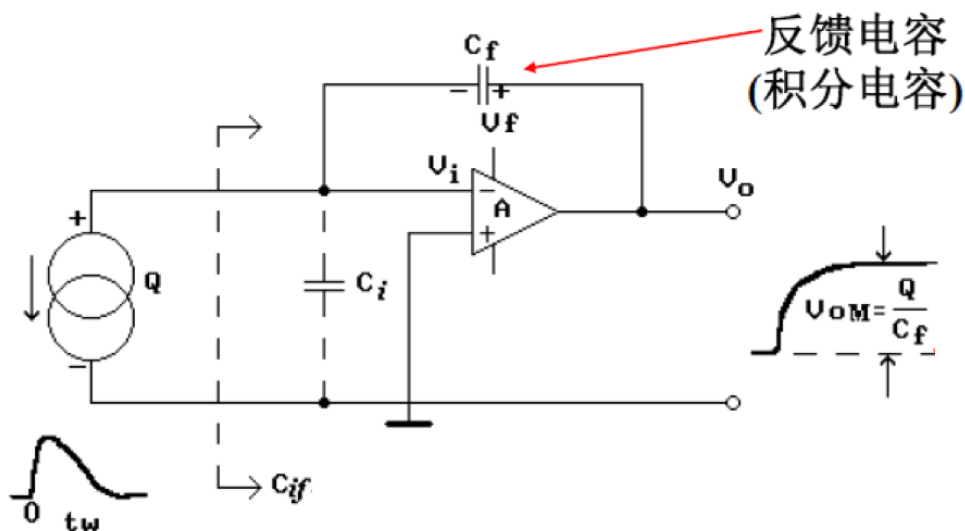


How is signal processed



电荷灵敏型前置放大器，以输出端开路为例

高输入阻抗，高放大倍数的负反馈倒相放大器，放大倍数为 $-A_0$ ，反馈电容为 C_f ，探测器与放大器输入端的总电容为 C_i



$$Q = \int_0^{+\infty} i_i dt. \text{ 输入总电荷}$$

$V_o = -A_0 V_i$ 输出端电压和输入端电压之间的关系，

由于反馈电路的存在，以及放大器的高阻抗，输入电流将分别流向 C_i 和 C_f ，分别形成电压为 V_i 和 $V_o - V_i$

电荷在两个电容上的分配为：

$$Q = V_i C_i + (V_o - V_i) C_f = \frac{V_o}{A_0} C_i + \left(V_o + \frac{V_o}{A_0} \right) C_f = V_o \left[\frac{C_i}{A_0} + \left(1 + \frac{1}{A_0} \right) C_f \right]$$

由于 A_0 很大: $Q = V_0 \left[\frac{C_i}{A_0} + \left(1 + \frac{1}{A_0} \right) C_f \right] \approx V_0 C_f$

可以得到稳定的输出电压和输入电荷的关系

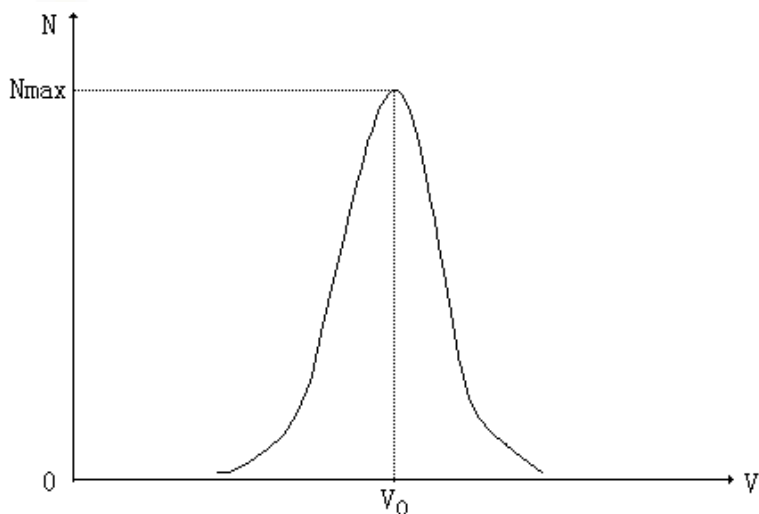
由于 C_i 受探测器分布电容的影响, 每个信号道 C_i 都有不同, 但是电荷灵敏放大器将不受该影响。

$Q = \frac{V_0}{A_0} A_0 C_f = V_i (-A_0 C_f)$ 对于输入端电压来说, 相当于输入电容为 $-A_0 C_f$, 为一个很大的值, 有利于电荷从探测器全部流向放大器

- ❖ 对于连续工作的电荷灵敏放大器, 与反馈电容并联一个电阻, 起到泄放电荷的作用, 一般取值为 10^8 — $10^9 \Omega$,

信号强度测量（电荷重心法）

需求：前放输出电压 $V \propto$ 探测器信号电荷量 Q



图(2-1-1) 幅度谱曲线

实际测量：

由峰位确定粒子能量；

由分布的宽度确定测量误差。

影响信号强度分辨的几个因素

- ◆ **探测器的固有分辨**：电离或激发过程中的涨落，电离电子和光子的收集效率的涨落，电子雪崩的涨落，方差为 σ_D 。某些探测器例如STAR TPC电离涨落的误差是主要的，大于电子学带来的噪音
- ◆ **噪声引起的谱线展宽**：电子学噪声随机涨落叠加在信号上，从而造成信号幅度的随机分布，加宽了能谱曲线。对能谱线展宽的方差贡献为 σ_n 。
- ◆ **堆积和基线涨落**：探测器产生的信号在时间上是随机的，因而有可能出现后面信号叠加前一个信号尾巴上的情况，对谱线方差贡献为 σ_p 。通过极零相消而缩短信号尾巴。
- ◆ **径迹亏损（弹道亏损）**：探测器电流脉冲并不是理想冲击信号，存在着一定宽度和一定形状，电子学对于不同宽度和形状的信号响应会有所不同，造成输出信号幅度波动，因而也会引起谱线展宽 σ_b 。

径迹亏损

输入电流 $i_D(t) = Q\delta(t)$ 时，电容瞬间充电，输出信号为电容电压泄放函数 $v_o(t) = \frac{Q}{C_i} (e^{-\frac{t}{\tau_i}})$ ， $v_o(t)$ 的最大值为 $v_{m\delta} = v_o(0) = \frac{Q}{C_i}$

实际的信号的持续时间不为0，电容充电的同时会泄放电荷，电压峰值 $v_{mT} < v_{m\delta}$ ，信号形状不同，还会带来 V_m 涨落，称为径迹亏损

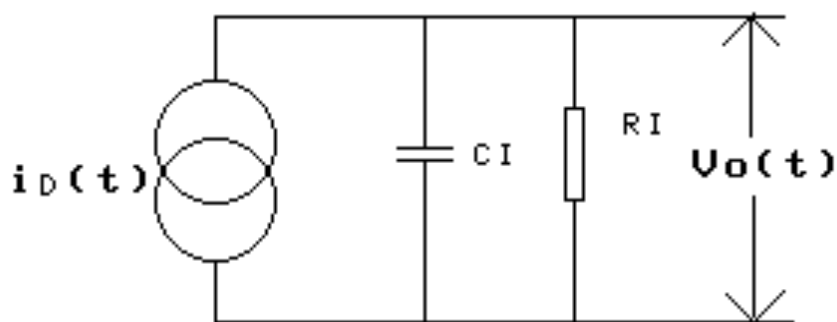
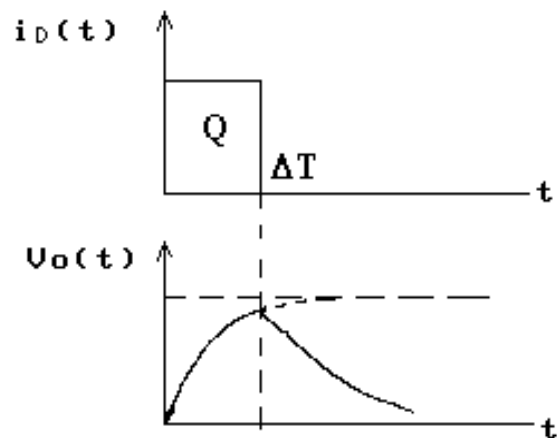


图 (2-1-3)



以输入方波电流信号为例：
$$i_D(t) = \begin{cases} \frac{Q}{T_d} & (t > 0, \quad t < T_d) \\ 0. & (t < 0, \quad t > T_d) \end{cases}$$

电子学的激励函数 $h(t)$ 为输入电流为 $\delta(t)$ 时的输出电压信号，那么一般的电压函数为电流函数和 $h(t)$ 的卷积：

$$v_o(t) = i_D(t) * h(t) = \int_{-\infty}^{+\infty} h(\tau) i_D(t - \tau) d\tau$$

相当于无穷多面积为 $i_D(t - \tau)d\tau$ 的 δ 函数引起的输出函数的叠加，在卷积函数中：

$$i_D(t - \tau) = \begin{cases} \frac{Q}{T_d} & (t - \tau > 0, t - \tau < T_d) \rightarrow (\tau < t, \tau > t - T_d) \\ 0. & (t - \tau < 0, t - \tau > T_d) \rightarrow (\tau > t, \tau < t - T_d) \end{cases}$$

因此
$$v_o(t) = \int_{t-T_d}^t h(\tau) i_D(t - \tau) d\tau = \frac{Q}{T_d} \int_{t-T_d}^t h(\tau) d\tau$$

$$v_o(0) = \frac{Q}{T_d} \int_{-T_d}^0 h(\tau) d\tau = 0$$

$$v_{o,end} = \frac{Q}{T_d} \int_{t_{h_end}}^{t_{h_end}+T_d} h(\tau) d\tau = 0$$



$$v_{o,max} = \frac{Q}{T_d} \int_{t_{max}-T_d}^{t_{max}} h(\tau) d\tau$$

输入电流 $Q\delta(t)$ 对应的输出信号为 $Qh(t)$, $v_{m\delta}$ 即为 Qh_m , 不存在径迹亏损

$$\text{定义径迹亏损 } D_B = 1 - \frac{V_{mT}}{V_{m\delta}} = 1 - \frac{\frac{Q}{T_d} \int_{t_{max}}^{t_{max}+T_d} h(\tau) d\tau}{Qh_m} = 1 - \frac{\int_{t_{max}}^{t_{max}+T_d} h(\tau) d\tau}{h_m T_d}$$

$D_B = \frac{S_2}{S_1+S_2}$. 电子学信号的激励函数 $h(t)$ 的顶端越平坦, 径迹亏损越小, 也更有利于数字化。

直观上讲, 响应函数能够保持一段时间不泄放电荷, 则可以防止径迹亏损

